

Probabilistic Forecasts, Calibration and Sharpness

Tilmann Gneiting^{1,2}, Fadoua Balabdaoui³ and Adrian E. Raftery¹

¹Department of Statistics, University of Washington
Seattle, Washington 98195-4322, USA

²Abteilung Bodenphysik, Universität Bayreuth
95440 Bayreuth, Germany

³Institut für Mathematische Stochastik, Georg-August-Universität Göttingen
37073 Göttingen, Germany

Technical Report no. 483
Department of Statistics, University of Washington

May 2005

Abstract

Probabilistic forecasts of a continuous variable take the form of predictive densities or predictive cumulative distribution functions. We propose a diagnostic approach to the evaluation of predictive performance that is based on the paradigm of *maximizing the sharpness of the predictive distributions subject to calibration*. Calibration refers to the statistical consistency between the distributional forecasts and the observations and is a joint property of the predictions and the events that materialize. Sharpness refers to the concentration of the predictive distributions and is a property of the forecasts only. A simple game-theoretic framework allows us to distinguish probabilistic calibration, exceedance calibration and marginal calibration. We propose and study tools for checking calibration and sharpness, among them the probability integral transform (PIT) histogram, marginal calibration plots, the sharpness diagram and proper scoring rules. The diagnostic approach is illustrated by an assessment and ranking of probabilistic forecasts of wind speed at the Stateline wind energy center in the US Pacific Northwest. In combination with cross-validation or in the time series context, our proposal provides very general, nonparametric alternatives to the use of information criteria for model diagnostics and model selection.

Keywords: Cross-validation; Density forecast; Ensemble prediction system; Forecast verification; Model diagnostics; Posterior predictive assessment; Predictive distribution; Prequential principle; Probability integral transform; Proper scoring rule

1 Introduction

A major human desire is to make forecasts for the future. Forecasts characterize and reduce but generally do not eliminate uncertainty. Consequently, forecasts should be probabilistic in nature, taking the form of probability distributions over future events (Dawid 1984). Indeed, over the past two decades the quest for good probabilistic forecasts has become a driving force in meteorology. Major economic forecasts such as the quarterly Bank of England inflation report are issued in terms of predictive distributions, and the rapidly growing area of financial risk management is dedicated

Report Documentation Page

Form Approved
OMB No. 0704-0188

Public reporting burden for the collection of information is estimated to average 1 hour per response, including the time for reviewing instructions, searching existing data sources, gathering and maintaining the data needed, and completing and reviewing the collection of information. Send comments regarding this burden estimate or any other aspect of this collection of information, including suggestions for reducing this burden, to Washington Headquarters Services, Directorate for Information Operations and Reports, 1215 Jefferson Davis Highway, Suite 1204, Arlington VA 22202-4302. Respondents should be aware that notwithstanding any other provision of law, no person shall be subject to a penalty for failing to comply with a collection of information if it does not display a currently valid OMB control number.

1. REPORT DATE MAY 2005	2. REPORT TYPE	3. DATES COVERED 00-05-2005 to 00-05-2005		
4. TITLE AND SUBTITLE Probabilistic Forecasts, Calibration and Sharpness		5a. CONTRACT NUMBER		
		5b. GRANT NUMBER		
		5c. PROGRAM ELEMENT NUMBER		
6. AUTHOR(S)		5d. PROJECT NUMBER		
		5e. TASK NUMBER		
		5f. WORK UNIT NUMBER		
7. PERFORMING ORGANIZATION NAME(S) AND ADDRESS(ES) University of Washington, Department of Statistics, Box 354322, Seattle, WA, 98195-4322		8. PERFORMING ORGANIZATION REPORT NUMBER		
9. SPONSORING/MONITORING AGENCY NAME(S) AND ADDRESS(ES)		10. SPONSOR/MONITOR'S ACRONYM(S)		
		11. SPONSOR/MONITOR'S REPORT NUMBER(S)		
12. DISTRIBUTION/AVAILABILITY STATEMENT Approved for public release; distribution unlimited				
13. SUPPLEMENTARY NOTES				
14. ABSTRACT				
15. SUBJECT TERMS				
16. SECURITY CLASSIFICATION OF:			17. LIMITATION OF ABSTRACT	
a. REPORT unclassified	b. ABSTRACT unclassified	c. THIS PAGE unclassified		
			18. NUMBER OF PAGES 31	19a. NAME OF RESPONSIBLE PERSON

to probabilistic forecasts of portfolio values (Duffie and Pan 1997). In the statistical literature, advances in Markov chain Monte Carlo methodology (see, for example, Besag, Green, Higdon and Mengersen 1995) have led to explosive growth in the use of predictive distributions, mostly in the form of Monte Carlo samples from the posterior predictive distribution of quantities of interest.

It is often crucial to assess the predictive ability of forecasters, or to compare and rank competing forecasting methods. Atmospheric scientists talk of *forecast verification* when they refer to this process (Jolliffe and Stephenson 2003), and much of the underlying methodology has been developed by meteorologists. There is also a relevant strand of work in the econometrics literature (Diebold and Mariano 1995; Christoffersen 1998; Diebold, Gunther and Tay 1998). Murphy and Winkler (1987) proposed a general framework for the evaluation of point forecasts that uses a diagnostic approach based on graphical displays, summary measures and scoring rules. In this paper, we consider probabilistic forecasts (as opposed to point forecasts) of continuous and mixed discrete-continuous variables, such as temperature, wind speed, precipitation, gross domestic product, inflation rates and portfolio values. In this situation, probabilistic forecasts take the form of predictive densities or predictive cumulative distribution functions, and the diagnostic approach faces a challenge, in that the forecasts take the form of probability distributions while the observations are real-valued.

We consider a simple game-theoretic framework for the evaluation of predictive performance. At times $t = 1, 2, \dots$, nature chooses a distribution, G_t , which we think of as the true data generating process, and the forecaster chooses a probabilistic forecast in the form of a predictive cumulative distribution function, F_t . The observation, x_t , is a random number with distribution G_t . If

$$F_t = G_t \quad \text{for all } t \tag{1}$$

we talk of a *perfect* forecaster. In practice, the true distribution, G_t , remains hypothetical, and the predictive distribution, F_t , is understood as an expert opinion which may or may not derive from a statistical prediction algorithm. In accordance with Dawid's (1984) *prequential principle*, the predictive distributions need to be assessed on the basis of the forecast-observation pairs (F_t, x_t) only, irrespective of their origins. Dawid (1984) and Diebold, Gunther and Tay (1998) proposed the use of the *probability integral transform* or PIT value,

$$p_t = F_t(x_t), \tag{2}$$

for doing this. If the forecaster is perfect and F_t is continuous, then p_t has a uniform distribution. Hence, the uniformity of the probability integral transform is a necessary condition for the forecaster to be perfect, and checks for its uniformity have formed a cornerstone of forecast evaluation, particularly in econometrics and meteorology. In the classical time series framework, each F_t corresponds to a one-step ahead forecast, and checks for the uniformity of the probability integral transform have been supplemented by checks for its independence (Frühwirth-Schnatter 1996; Diebold et al. 1998).

Hamill (2001) gave a thought-provoking example of a forecaster for whom the histogram of the PIT values is essentially uniform, even though every single probabilistic forecast is biased. His example aimed to show that the uniformity of the PIT values is a necessary but not a sufficient condition for the forecaster to be perfect. To fix the idea, we consider a simulation study based on the scenario described in Table 1. At times $t = 1, 2, \dots$, nature chooses the distribution $G_t = \mathcal{N}(\mu_t, 1)$ where μ_t is standard normal. In the context of weather forecasts, we might think of μ_t as an accurate description of the latest observable state of the atmosphere. The perfect forecaster is an expert meteorologist who conditions on the current state, μ_t , and issues a perfect probabilistic

Table 1: Scenario for the simulation study. At times $t = 1, 2, \dots$, nature chooses a distribution, G_t , the forecaster chooses a probabilistic forecast, F_t , and the observation is a random number, x_t , with distribution G_t . We write $\mathcal{N}(\mu, \sigma^2)$ for the normal distribution with mean μ and variance σ^2 , and we identify distributions and cumulative distribution functions, respectively. The sequences $(\mu_t)_{t=1,2,\dots}$, $(\tau_t)_{t=1,2,\dots}$ and $(\delta_t, \sigma_t^2)_{t=1,2,\dots}$ are independent identically distributed and independent of each other.

Nature	$G_t = \mathcal{N}(\mu_t, 1)$ where $\mu_t \sim \mathcal{N}(0, 1)$
Perfect forecaster	$F_t = \mathcal{N}(\mu_t, 1)$
Climatological forecaster	$F_t = \mathcal{N}(0, 2)$
Unfocused forecaster	$F_t = \frac{1}{2} (\mathcal{N}(\mu_t, 1) + \mathcal{N}(\mu_t + \tau_t, 1))$ where $\tau_t = \pm 1$ with probability $\frac{1}{2}$ each
Hamill's forecaster	$F_t = \mathcal{N}(\mu_t + \delta_t, \sigma_t^2)$ where $(\delta_t, \sigma_t^2) = (\frac{1}{2}, 1), (-\frac{1}{2}, 1)$ or $(0, \frac{169}{100})$ with probability $\frac{1}{3}$ each

forecast, $F_t = G_t$. The climatological forecaster takes the unconditional distribution, $F_t = \mathcal{N}(0, 2)$, as probabilistic forecast. The unfocused forecaster observes the current state, μ_t , but adds a mixture component to the forecast, which can be interpreted as distributional bias. A similar comment applies to Hamill's forecaster. Clearly, our forecasters are caricatures of operational weather forecasters; yet, climatological reference forecasts and conditional biases are frequently observed in practice. For simplicity, we assume that the states, μ_t , are independent. Extensions to serially dependent states are straightforward and will be discussed below. The observation, x_t , is a random draw from G_t , and we repeat the prediction experiment 10000 times. Figure 1 shows that the PIT histograms for the four forecasters are essentially uniform; furthermore, the PIT values are independent, and this remains true under serially dependent states, with the single exception of the climatological forecaster. The respective sample autocorrelation functions are illustrated in Figures 2 and 3.

In view of the reliance on the probability integral transform in the extant literature, this is a disconcerting result. As Diebold, Gunther and Tay (1998) pointed out, the perfect forecaster is preferred by all users, regardless of the respective loss function. Yet, the probability integral transform is unable to distinguish between the perfect forecaster and her competitors. To address these limitations, we propose a diagnostic approach to the evaluation of predictive performance that is based on the paradigm of *maximizing the sharpness of the predictive distributions subject to calibration*. Calibration refers to the statistical consistency between the distributional forecasts and the observations, and is a joint property of the predictions and the observed values. Sharpness refers to the concentration of the predictive distributions and is a property of the forecasts only. The more concentrated the predictive distributions, the sharper the forecasts, and the sharper the better, subject to calibration.

The remainder of the paper is organized as follows. Section 2 develops our game-theoretic

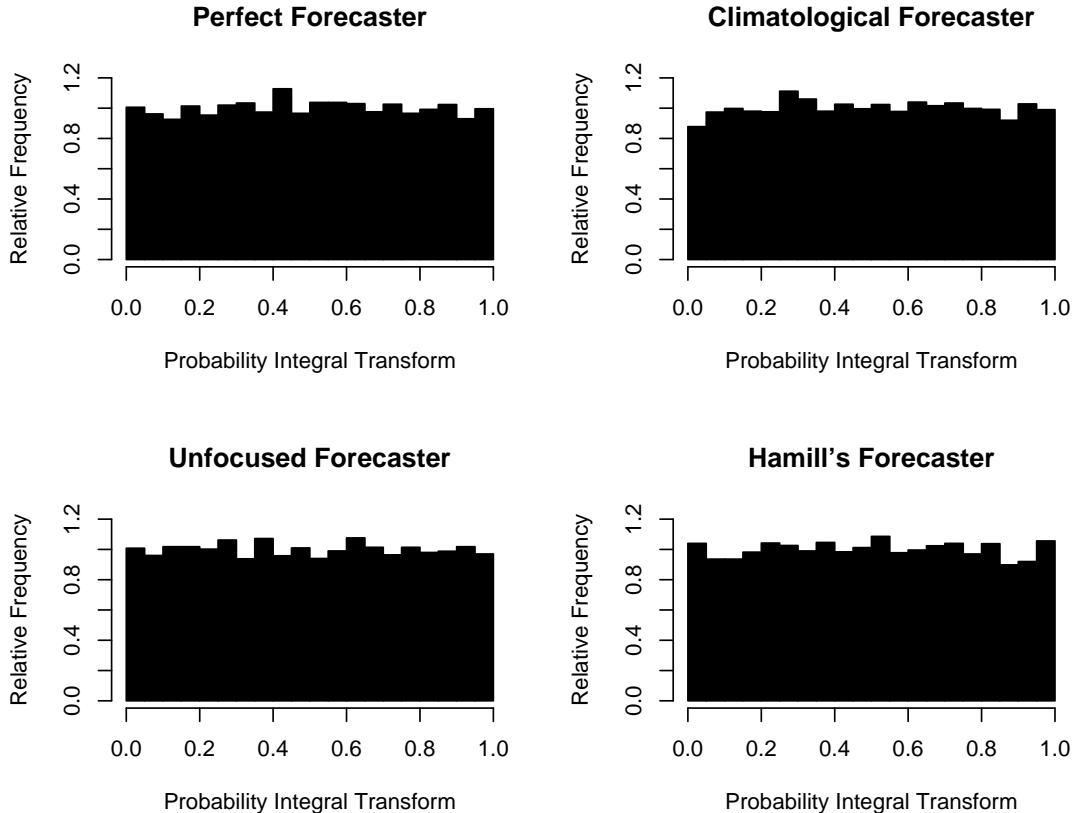


Figure 1: Probability integral transform (PIT) histograms.

framework for the assessment of predictive performance. We introduce the notions of probabilistic calibration, exceedance calibration and marginal calibration, give examples and counterexamples, and discuss a conjectured sharpness principle. In Section 3, we propose diagnostic tools such as marginal calibration plots and sharpness diagrams that complement the PIT histogram. Proper scoring rules address calibration as well as sharpness and allow for the ranking of competing forecast procedures. Section 4 turns to a case study on probabilistic forecasts at the Stateline wind energy center in the US Pacific Northwest. The diagnostic approach yields a clear-cut ranking of statistical algorithms for forecasts of wind speed, and suggests forecast improvements that can be addressed in future research. Similar approaches hold considerable promise as very general, nonparametric tools for statistical model selection and model diagnostics. The paper closes with a discussion in Section 5 that emphasizes the need for routine assessments of sharpness in the evaluation of predictive performance.

2 Modes of calibration

We consider probabilistic forecasting as a game played between nature and the forecaster. At times or instances $t = 1, 2, \dots$, nature chooses a distribution, G_t , and the forecaster chooses a probabilistic forecast in the form of a predictive cumulative distribution function, F_t . The observation, x_t , is a

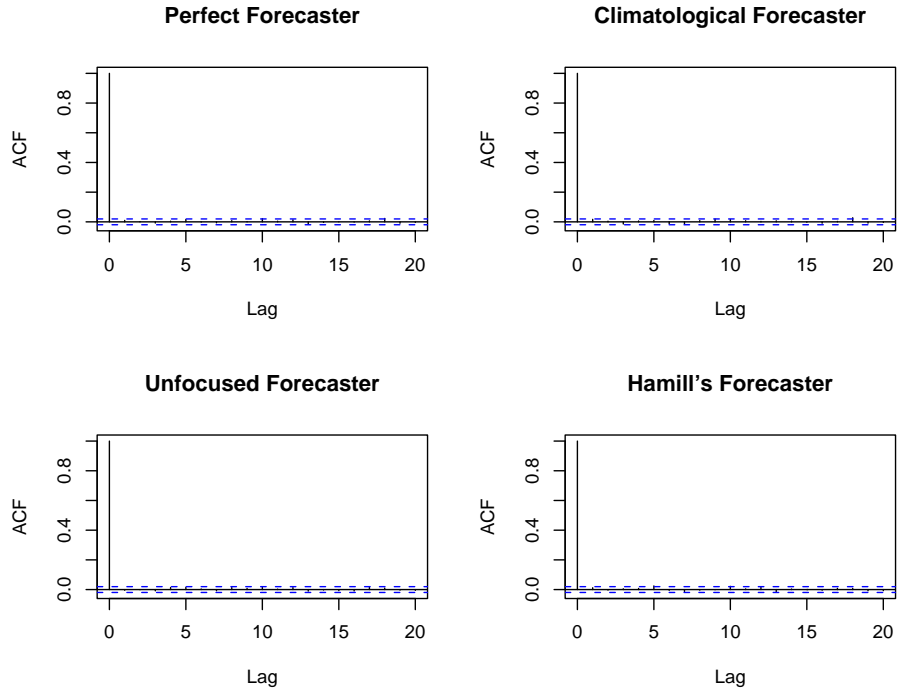


Figure 2: Sample autocorrelation functions for the probability integral transform.

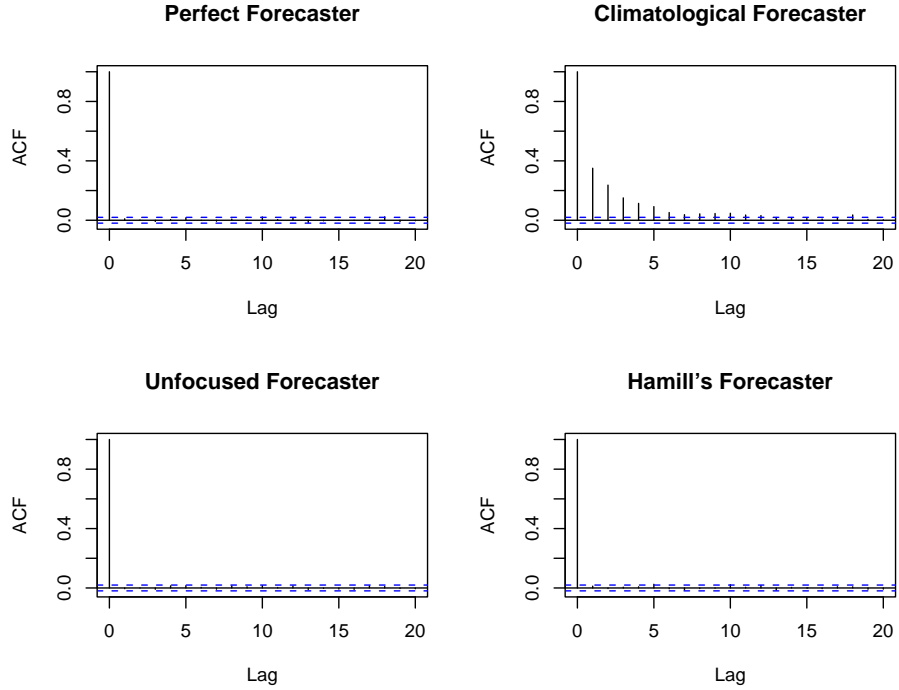


Figure 3: Same as Figure 2 except that the states, μ_t , are now serially dependent, following a stationary Gaussian autoregression of order 1 with autoregressive parameter $\frac{1}{2}$.

random number with distribution G_t . For simplicity, we suppose that F_t and G_t are continuous and strictly increasing on \mathbb{R} . In this framework, calibration refers to the asymptotic compatibility of the sequences $(G_t)_{t=1,2,\dots}$ and $(F_t)_{t=1,2,\dots}$, which correspond to the data generating mechanism and to the forecasts, respectively. Our approach seems slightly broader than Dawid's (1984) prequential framework, since we think of $(F_t)_{t=1,2,\dots}$ as a general, countable sequence of forecasts, with the index referring to time, space or subjects, depending on the prediction problem at hand.

2.1 Probabilistic calibration, exceedance calibration and marginal calibration

Henceforth, $(F_t)_{t=1,2,\dots}$ and $(G_t)_{t=1,2,\dots}$ denote sequences of continuous and strictly increasing cumulative distribution functions, possibly depending on stochastic parameters. We think of $(G_t)_{t=1,2,\dots}$ as the true data generating process and of $(F_t)_{t=1,2,\dots}$ as the associated sequence of probabilistic forecasts. The following definition refers to the asymptotic compatibility between the data generating process and the predictive distributions in terms of three major modes of calibration. Given that $(F_t)_{t=1,2,\dots}$ and $(G_t)_{t=1,2,\dots}$ might depend on stochastic parameters, convergence is understood as almost sure convergence and is denoted by an arrow.

Definition 1 (modes of calibration)

- (a) The sequence $(F_t)_{t=1,2,\dots}$ is *probabilistically calibrated* relative to the sequence $(G_t)_{t=1,2,\dots}$ if

$$\frac{1}{T} \sum_{t=1}^T G_t \circ F_t^{-1}(p) \longrightarrow p \quad \text{for all } p \in (0, 1). \quad (3)$$

- (b) The sequence $(F_t)_{t=1,2,\dots}$ is *exceedance calibrated* relative to $(G_t)_{t=1,2,\dots}$ if

$$\frac{1}{T} \sum_{t=1}^T G_t^{-1} \circ F_t(x) \longrightarrow x \quad \text{for all } x \in \mathbb{R}. \quad (4)$$

- (c) The sequence $(F_t)_{t=1,2,\dots}$ is *marginally calibrated* relative to $(G_t)_{t=1,2,\dots}$ if the limits $\bar{G}(x) = \lim_{T \rightarrow \infty} \frac{1}{T} \sum_{t=1}^T G_t(x)$ and $\bar{F}(x) = \lim_{T \rightarrow \infty} \frac{1}{T} \sum_{t=1}^T F_t(x)$ exist and equal each other for all $x \in \mathbb{R}$, and if the common limit distribution places all mass on finite values.
- (d) The sequence $(F_t)_{t=1,2,\dots}$ is *strongly calibrated* relative to $(G_t)_{t=1,2,\dots}$ if it is probabilistically calibrated, exceedance calibrated and marginally calibrated.

If each subsequence of $(F_t)_{t=1,2,\dots}$ is probabilistically calibrated relative to the associated subsequence of $(G_t)_{t=1,2,\dots}$, we talk of *complete* probabilistic calibration. Similarly, we define completeness for exceedance calibration, marginal calibration and strong calibration. In the examples below, calibration will generally be complete. Probabilistic calibration is essentially equivalent to the uniformity of the probability integral transform. Exceedance calibration is defined in terms of thresholds, and marginal calibration requires that the limit distributions \bar{G} and \bar{F} exist and equal each other. The existence of \bar{G} is a natural assumption in meteorological problems and corresponds to the existence of a stable climate. Hence, marginal calibration can be interpreted in terms of the equality of actual climatology and forecast climatology.

Various authors have studied calibration in the context of probability forecasts for sequences of binary events (Dawid 1982, 1985a, 1985b; Oakes 1985; Schervish 1985, 1989). The progress

is impressive and culminates in the paper by Foster and Vohra (1998), who viewed the prediction problem as a game played against nature as well. Krzysztofowicz (1999) discussed calibration in the context of Bayesian forecasting systems, and Krzysztofowicz and Sigrest (1999) studied calibration for quantile forecasts of quantitative precipitation. However, we are unaware of any prior discussion of notions of calibration for probabilistic forecasts of continuous variables.

2.2 Examples

The examples in this section illustrate the aforementioned modes of calibration and discuss some of the forecasters in our initial simulation study. Unless noted otherwise, $(\mu_t)_{t=1,2,\dots}$, $(\sigma_t)_{t=1,2,\dots}$ and $(\tau_t)_{t=1,2,\dots}$ denote independent sequences of independent identically distributed random variables. We write $\mathcal{N}(\mu, \sigma^2)$ for the normal distribution with mean μ and variance σ^2 , identify distributions and cumulative distribution functions, respectively, and let Φ denote the standard normal cumulative.

Example 1 (climatological forecaster)

$$G_t = \mathcal{N}(\mu_t, 1) \text{ where } \mu_t \sim \mathcal{N}(0, 1)$$

$$F_t = \mathcal{N}(0, 2) \text{ for all } t$$

The climatological forecaster is probabilistically calibrated and marginally calibrated, but not exceedance calibrated. The claim for marginal calibration is obvious. Putting $p = F_t(x)$ in (3), we see that probabilistic calibration holds, too. However,

$$\frac{1}{T} \sum_{t=1}^T G_t^{-1} \circ F_t(x) = \frac{1}{T} \sum_{t=1}^T \left[\Phi^{-1} \left(\Phi \left(\frac{x}{\sqrt{2}} \right) \right) + \mu_t \right] \longrightarrow \frac{x}{\sqrt{2}}$$

for $x \in \mathbb{R}$, in violation of exceedance calibration.

The characteristic property in Example 1 is that the predictive distributions, F_t , all equal nature's limiting distribution, \bar{G} . We call any forecaster with this property a *climatological* forecaster. For climatological forecasts, probabilistic calibration is essentially equivalent to marginal calibration. Indeed, if \bar{G} is continuous and strictly increasing, then putting $p = F_t(x) = \bar{G}(x)$ in (3) recovers the marginal calibration condition. In practice, climatological forecasts are constructed from historical records of the observations, and they are often used as reference forecasts.

Example 2 (unfocused forecaster)

$$G_t = \mathcal{N}(\mu_t, 1) \text{ where } \mu_t \sim \mathcal{N}(0, 1)$$

$$F_t = \frac{1}{2} (\mathcal{N}(\mu_t, 1) + \mathcal{N}(\mu_t + \tau_t, 1)) \text{ where } \text{pr}(\tau_t = \pm 1) = \frac{1}{2}$$

The unfocused forecaster is probabilistically calibrated relative to $(G_t)_{t=1,2,\dots}$, but neither exceedance calibrated nor marginally calibrated. To prove the claim for probabilistic calibration, put $\Phi_{\pm}(x) = \frac{1}{2}(\Phi(x) + \Phi(x \mp 1))$ and note that

$$\frac{1}{T} \sum_{t=1}^T G_t \circ F_t^{-1}(p) \longrightarrow \frac{1}{2} \left[\Phi \circ \Phi_+^{-1}(p) + \Phi \circ \Phi_-^{-1}(p) \right] = p,$$

where the equality follows upon putting $p = \Phi_+(x)$, substituting and simplifying. Exceedance calibration does not hold, because

$$\frac{1}{T} \sum_{t=1}^T G_t^{-1} \circ F_t(x) \longrightarrow \frac{1}{2} \left[\Phi^{-1} \circ \Phi_+(x) + \Phi^{-1} \circ \Phi_-(x) \right] \neq x$$

in general. The marginal calibration condition is violated, because nature's limit distribution, $\bar{G} = \mathcal{N}(0, 2)$, does not equal $\bar{F} = \frac{1}{2}\mathcal{N}(0, 2) + \frac{1}{4}\mathcal{N}(-1, 2) + \frac{1}{4}\mathcal{N}(1, 2)$.

Example 3 (sign-biased forecaster)

$$G_t = \mathcal{N}(\tau_t, 1) \text{ where } \text{pr}(\tau_t = \pm 1) = \frac{1}{2}$$

$$F_t = \mathcal{N}(-\tau_t, 1)$$

The sign-biased forecaster is exceedance calibrated and marginally calibrated, but not probabilistically calibrated. Specifically,

$$\frac{1}{T} \sum_{t=1}^T G_t \circ F_t^{-1}(p) \longrightarrow \frac{1}{2} \left[\Phi \left(\Phi^{-1}(p) - 2 \right) + \Phi \left(\Phi^{-1}(p) + 2 \right) \right] \neq p$$

in general. However,

$$\frac{1}{T} \sum_{t=1}^T G_t^{-1} \circ F_t(x) \longrightarrow \frac{1}{2} \left[(x + 2) + (x - 2) \right] = x$$

for $x \in \mathbb{R}$. The claim for marginal calibration is obvious.

Example 4 (mean-biased forecaster)

$$G_t = \mathcal{N}(\mu_t, 1) \text{ where } \mu_t \sim \mathcal{N}(0, 1)$$

$$F_t = \mathcal{N}(\mu_t + \tau_t, 1) \text{ where } \text{pr}(\tau_t = \pm 1) = \frac{1}{2}$$

The mean-biased forecaster is exceedance calibrated but neither probabilistically calibrated nor marginally calibrated. Specifically,

$$\frac{1}{T} \sum_{t=1}^T G_t \circ F_t^{-1}(p) \longrightarrow \frac{1}{2} \left[\Phi \left(\Phi^{-1}(p) - 1 \right) + \Phi \left(\Phi^{-1}(p) + 1 \right) \right] \neq p$$

in general, while

$$\frac{1}{T} \sum_{t=1}^T G_t^{-1} \circ F_t(x) \longrightarrow \frac{1}{2} \left[(x + 1) + (x - 1) \right] = x$$

for $x \in \mathbb{R}$. The marginal calibration condition does not hold, because nature's limit distribution, $\bar{G} = \mathcal{N}(0, 2)$, differs from $\bar{F} = \frac{1}{2}(\mathcal{N}(-1, 2) + \mathcal{N}(1, 2))$.

We now return to the climatological forecaster in Example 1, with the roles of nature and the forecaster interchanged.

Table 2: The three major modes of calibration are logically independent of each other and may occur in any combination. For instance, the sign-biased forecaster in Example 3 is exceedance calibrated (E) and marginally calibrated (M) but not probabilistically calibrated (\bar{P}).

Properties	Example
PEM	$F_t = G_t = \mathcal{N}(0, 1)$
PE \bar{M}	$F_t = G_t = \mathcal{N}(t, 1)$
P \bar{E} M	Example 1 (climatological forecaster)
P \bar{E} \bar{M}	Example 2 (unfocused forecaster)
\bar{P} EM	Example 3 (sign-biased forecaster)
\bar{P} E \bar{M}	Example 4 (mean-biased forecaster)
\bar{P} \bar{E} M	Example 5 (reverse climatological forecaster)
\bar{P} \bar{E} \bar{M}	$G_t = \mathcal{N}(t, 1); F_t = \mathcal{N}(-t, 1)$

Example 5 (reverse climatological forecaster)

$G_t = \mathcal{N}(0, 2)$ for all t

$F_t = \mathcal{N}(\mu_t, 1)$ where $\mu_t \sim \mathcal{N}(0, 1)$

The reverse climatological forecaster is marginally calibrated, but neither probabilistically calibrated nor exceedance calibrated. To prove the claim for probabilistic calibration, let Z be a standard normal random variable and note that

$$\begin{aligned} \frac{1}{T} \sum_{t=1}^T G_t \circ F_t^{-1}(p) &= \frac{1}{T} \sum_{t=1}^T \Phi\left(\frac{\Phi^{-1}(p) + \mu_t}{\sqrt{2}}\right) \\ &\longrightarrow \mathbb{E}\left[\Phi\left(\frac{\Phi^{-1}(p) + Z}{\sqrt{2}}\right)\right] = \int_{-\infty}^{\infty} \varphi(z) \Phi\left(\frac{\Phi^{-1}(p) - z}{\sqrt{2}}\right) dz \neq p \end{aligned}$$

in general. Exceedance calibration does not hold, because

$$\frac{1}{T} \sum_{t=1}^T G_t^{-1} \circ F_t(x) = \frac{1}{T} \sum_{t=1}^T \sqrt{2} \Phi^{-1}(\Phi(x - \mu_t)) \longrightarrow \sqrt{2} x$$

for $x \in \mathbb{R}$. The claim for marginal calibration is obvious.

The examples in this section show that probabilistic calibration, exceedance calibration and marginal calibration are logically independent of each other and may occur in any combination. Table 2 summarizes the respective results.

2.3 Hamill's forecaster

We add a discussion of Hamill's forecaster. As described in Table 1, Hamill's forecaster is a master forecaster who assigns the prediction task with equal probability to any of three student forecasters,

each of whom is biased. In response to nature's choice, $G_t = \mathcal{N}(\mu_t, 1)$, the student forecasters issue the predictive distributions $F_t = \mathcal{N}(\mu_t - \frac{1}{2}, 1)$, $F_t = \mathcal{N}(\mu_t + \frac{1}{2}, 1)$ and $F_t = \mathcal{N}(\mu_t, \frac{169}{100})$, respectively.

For Hamill's forecaster,

$$\frac{1}{T} \sum_{t=1}^T G_t \circ F_t^{-1}(p) \longrightarrow \frac{1}{3} \left[\Phi\left(\Phi^{-1}(p) - \frac{1}{2}\right) + \Phi\left(\frac{13}{10}\Phi^{-1}(p)\right) + \Phi\left(\Phi^{-1}(p) + \frac{1}{2}\right) \right] = p + \epsilon(p)$$

where $|\epsilon(p)| \leq 0.0032$ for all p but $\epsilon(p) \neq 0$ in general. The probabilistic calibration condition (3) is violated, but only slightly so, resulting in deceptively uniform histograms of the probability integral transforms. As for exceedance calibration, note that

$$\frac{1}{T} \sum_{t=1}^T G_t^{-1} \circ F_t(p) \longrightarrow \frac{1}{3} \left[\left(x + \frac{1}{2}\right) + \frac{10}{13}x + \left(x - \frac{1}{2}\right) \right] = \frac{12}{13}x$$

for $x \in \mathbb{R}$. Hence, Hamill's forecaster is not exceedance calibrated either, nor marginally calibrated, given that $\bar{G} = \mathcal{N}(0, 2)$ while $\bar{F} = \frac{1}{3}(\mathcal{N}(-\frac{1}{2}, 2) + \mathcal{N}(\frac{1}{2}, 2) + \mathcal{N}(0, \frac{269}{100}))$.

2.4 Sharpness principle

Ideally, probabilistic forecasts aim to honor the data generating process, resulting in the equality (1) of nature's proposal distribution, G_t , and the predictive distribution, F_t , that characterizes the perfect forecaster. Operationally, we adopt the paradigm of maximizing the sharpness of the predictive distributions subject to calibration. Our conjectured *sharpness principle* contends that the two goals — perfect forecasts and the maximization of sharpness subject to calibration — are indeed equivalent. This conjectured equivalence could be explained in two distinct ways. One explanation is that sufficiently strong notions of calibration imply asymptotic equivalence to the perfect forecaster. We are unaware of any strongly calibrated forecasts that are not minor variants of perfect forecasts, and it would be interesting to find such an example, or to prove that sequences of this type do not exist. An alternative and weaker explanation states that any sufficiently calibrated forecaster is at least as spread out as the perfect forecaster.

With respect to this latter explanation, none of probabilistic, exceedance or marginal calibration alone is sufficiently stark. In the examples below it will be convenient to consider a probabilistic calibration condition,

$$\frac{1}{T} \sum_{t=1}^T G_t \circ F_t^{-1}(p) = p \quad \text{for all } p \in (0, 1), \quad (5)$$

for finite sequences $(F_t)_{1 \leq t \leq T}$ relative to $(G_t)_{1 \leq t \leq T}$, and similarly for exceedance calibration and marginal calibration. Using randomization, the examples extend to countable sequences in obvious ways. Now suppose that $\sigma > 0$, $a > 1$, $0 < \lambda < 1/a$ and $T = 2$. Let G_1 and G_2 be continuous and strictly increasing distributions functions with associated densities that are symmetric about zero and have finite variance, $\text{var}(G_1) = \sigma^2$ and $\text{var}(G_2) = \lambda\sigma^2$. If we define

$$F_1(x) = \frac{1}{2} \left(G_1(x) + G_2\left(\frac{x}{a}\right) \right), \quad F_2(x) = F_1(ax),$$

then

$$\text{var}(F_1) + \text{var}(F_2) = \frac{1}{2} \left(1 + \frac{1}{a^2} \right) (1 + a^2\lambda^2) \sigma^2 < (1 + \lambda^2) \sigma^2 = \text{var}(G_1) + \text{var}(G_2),$$

even though the finite probabilistic calibration condition (5) holds. A similar example can be given for exceedance calibration. Suppose that $\sigma > 0$, $0 < a < 1$ and

$$0 < \lambda < a \left(\frac{3+a}{1+3a} \right)^{1/2}.$$

Let G_1 and G_2 be as above and define

$$F_1(x) = G_1\left(\frac{2x}{1+a}\right), \quad F_2(x) = G_2\left(\frac{2ax}{1+a}\right).$$

Then

$$\text{var}(F_1) + \text{var}(F_2) = \frac{1}{4}(1+a)^2 \left(1 + \frac{\lambda^2}{a^2}\right) \sigma^2 < (1+\lambda^2) \sigma^2 = \text{var}(G_1) + \text{var}(G_2).$$

even though the finite exceedance calibration condition holds. Finally, the reverse climatological forecaster shows that a forecaster can be marginally calibrated yet sharper than the perfect forecaster.

For climatological forecasts, however, finite probabilistic calibration and finite marginal calibration are equivalent, and a weak form of the sharpness principle holds.

Theorem 1 Suppose that G_1, \dots, G_T and $F_1 = \dots = F_T = F$ have second moments and satisfy the finite probabilistic calibration condition (5). Then

$$\frac{1}{T} \sum_{t=1}^T \text{var}(F_t) = \text{var}(F) \geq \frac{1}{T} \sum_{t=1}^T \text{var}(G_t)$$

with equality if and only if $E(G_1) = \dots = E(G_T)$.

The proof of Theorem 1 is given in the appendix. We are unaware of any other results in this direction; in particular, we do not know whether a non-climatological forecaster can be probabilistically calibrated and marginally calibrated yet sharper than the perfect forecaster.

3 Diagnostic tools

We now discuss diagnostic tools for the evaluation of predictive performance. In accordance with Dawid's (1984) prequential principle, the assessment of probabilistic forecasts needs to be based on the predictive distributions and the observations only. Previously, we defined notions of calibration in terms of the asymptotic consistency between the probabilistic forecasts and the data generating distributions, which are unavailable in practice. However, we obtain sample versions by substituting empirical distribution functions based on the observations. In the following, this program is carried out for probabilistic calibration and marginal calibration. Probabilistic calibration is essentially equivalent to the uniformity of the probability integral transform, and marginal calibration corresponds to the equality of observed climate and forecast climate. Exceedance calibration does not allow for a sample analogue, given the ambiguities in inverting a step function. We discuss graphical displays of sharpness and propose the use of proper scoring rules, that assign numerical measures of predictive performance, address calibration as well as sharpness, and find key applications in the ranking of competing forecast procedures.

3.1 Assessing probabilistic calibration

The probability integral transform (PIT) is the value that the predictive cumulative distribution function attains at the observation. Specifically, if F_t is the predictive distribution and x_t materializes, the transform is defined as $p_t = F_t(x_t)$. The literature usually refers to Rosenblatt (1952), even though the probability integral transform can be traced back at least to Pearson (1933). The connection to probabilistic calibration is established by substituting the empirical distribution function $\mathbf{1}\{x_t \leq x\}$ for the data generating distribution $G_t(x)$, $x \in \mathbb{R}$ in the probabilistic calibration condition (3), and noting that the indicator functions $\mathbf{1}\{x_t \leq F_t^{-1}(p)\}$ and $\mathbf{1}\{p_t \leq p\}$ are identical. The following theorem characterizes the asymptotic uniformity of the empirical sequence of probability integral transforms in terms of probabilistic calibration. We state this result under the assumption of a *-mixing sequence of observations (Blum, Hanson and Koopmans 1963).

Theorem 2 Let $(F_t)_{t=1,2,\dots}$ and $(G_t)_{t=1,2,\dots}$ be sequences of continuous, strictly increasing distribution functions. Suppose that x_t has distribution G_t and that the x_t form a *-mixing sequence of random variables. Then

$$\frac{1}{T} \sum_{t=1}^T \mathbf{1}\{p_t < p\} \longrightarrow p \quad \text{almost surely for all } p \quad (6)$$

if and only if $(F_t)_{t=1,2,\dots}$ is probabilistically calibrated with respect to $(G_t)_{t=1,2,\dots}$.

The proof of this result is given in the appendix, and the equivalence remains valid under alternative weak dependence assumptions for the observations. Essentially, the theorem states that the asymptotic uniformity of the PIT histogram is a necessary and sufficient condition for probabilistic calibration. Indeed, following the lead of Dawid (1984) and Diebold, Gunther and Tay (1998), checks for the uniformity of the PIT values have formed a cornerstone of forecast evaluation.

Uniformity is usually evaluated in an exploratory sense, and one way of doing this is by plotting the empirical cumulative distribution function of the PIT values and comparing to the identity function. This approach is adequate for small sample sizes and notable departures from uniformity, and its proponents include Staël von Holstein (1970, p. 142), Seillier-Moiseiwitsch (1993), Hoeting (1994, p. 33), Frühwirth-Schnatter (1996), Clements and Smith (2000), Moyeed and Parpritz (2002), Wallis (2003) and Boero and Marrocu (2004). Histograms of the probability integral transform accentuate departures from uniformity when the sample size is large and the deviations from uniformity are small. This alternative type of display was used by Diebold, Gunther and Tay (1998), Weigend and Shi (2000), Bouwens, Giot, Grammig and Veredas (2004) and Gneiting, Raftery, Westveld and Goldman (2005), among others, and 10 or 20 histogram bins generally seem adequate. Figure 1 uses 20 bins and shows the PIT histograms for the various forecasters in our initial simulation study. The histograms are essentially uniform. Table 3 shows the empirical coverage of the associated central 50% and 90% prediction intervals. This information is redundant, since the empirical coverage can be read off the PIT histogram, namely as the area under the 10 and 18 central bins, respectively.

Probabilistic weather forecasts are typically based on ensemble prediction systems, which generate a set of perturbations of the best estimate of the current state of the atmosphere, run each of them forward in time using a numerical weather prediction model, and use the resulting set of forecasts as a sample from the predictive distribution of future weather quantities (Palmer 2002). The

Table 3: Empirical coverages of central prediction intervals. The nominal coverages are 50% and 90%, respectively.

Interval	50%	90%
Perfect forecaster	51.2%	90.0%
Climatological forecaster	51.3%	90.7%
Unfocused forecaster	50.1%	90.1%
Hamill's forecaster	50.9%	89.5%

principal device for assessing the calibration of ensemble forecasts is the verification rank histogram or Talagrand diagram, proposed independently by Anderson (1996), Hamill and Colucci (1997) and Talagrand, Vautard and Strauss (1997), and extensively used since. To obtain a verification rank histogram, find the rank of the observation when pooled within the ordered ensemble values and plot the histogram of the ranks. If we identify the predictive distribution with the empirical cumulative distribution function of the ensemble values, this technique is seen to be equivalent to plotting a PIT histogram. A similar procedure could be drawn on fruitfully to assess samples from posterior predictive distributions obtained by Markov chain Monte Carlo techniques. Shephard (1994, p. 129) gave an instructive example of how this could be done.

Visual inspection of a PIT or rank histogram often provides hints to the reasons for forecast deficiency. Hump shaped histograms indicate overdispersed predictive distributions with prediction intervals that are too wide on average. U-shaped histograms often correspond to predictive distributions that are too narrow. Triangle-shaped histograms are seen when the predictive distributions are biased. Formal tests of uniformity can also be employed and have been studied by Anderson (1996), Talagrand, Vautard and Strauss (1997), Noceti, Smith and Hodges (2003), Wallis (2003) and Garratt, Lee, Pesaran and Shin (2003), among others. However, the use of formal tests is often hindered by complex dependence structures, particularly in cases in which the probability integral transforms are spatially aggregated. Hamill (2001) gave a thoughtful discussion of the associated issues and potential fallacies.

In the context of time series, the observations are sequential, and the predictive distributions correspond to sequential k -step ahead forecasts. The probability integral transforms for perfect k -step ahead forecasts are at most $(k - 1)$ -dependent, and this assumption can be checked empirically, by plotting the sample autocorrelation function for the PIT values and the higher moments thereof. This approach was applied by Diebold, Gunther and Tay (1998), Weigend and Shi (2000), Bauwens et al. (2004) and Campbell and Diebold (2005), among others. Figures 2 and 3 show the sample autocorrelation functions for the PIT values and the various forecasters in our initial simulation study, for independent states, μ_t , and for serially dependent states, respectively. Smith (1985), Frühwirth-Schnatter (1996) and Berkowitz (2001) proposed an assessment of independence based on the transformed PIT values, $\Phi^{-1}(p_t)$, which are Gaussian under the assumption of perfect forecasts. This further transformation has obvious advantages when formal tests of independence are employed, and seems to make little difference otherwise.

3.2 Assessing marginal calibration

Marginal calibration concerns the equality of actual climate and forecast climate. To assess marginal calibration, we propose a comparison of the empirical cumulative distribution function,

$$\hat{G}_T(x) = \frac{1}{T} \sum_{t=1}^T \mathbf{1}\{x_t \leq x\}, \quad x \in \mathbb{R}, \quad (7)$$

to the forecast climate, represented by the average predictive cumulative distribution function,

$$\bar{F}_T(x) = \frac{1}{T} \sum_{t=1}^T F_t(x), \quad x \in \mathbb{R}. \quad (8)$$

Indeed, if we substitute the indicator function $\mathbf{1}\{x_t \leq x\}$ for the data generating distribution $G_t(x)$, $x \in \mathbb{R}$ in the definition of marginal calibration, we are led to the asymptotic equality of \hat{G}_T and \bar{F}_T , respectively. Theorem 3 provides a rigorous version of this correspondence. Under mild regularity conditions, marginal calibration is a necessary and sufficient condition for the asymptotic equality of \hat{G}_T and \bar{F}_T . The proof of this result is deferred to the appendix.

Theorem 3 Let $(F_t)_{t=1,2,\dots}$ and $(G_t)_{t=1,2,\dots}$ be sequences of continuous, strictly increasing distribution functions. Suppose that each x_t has distribution G_t and that the x_t form a $*$ -mixing sequence of random variables. Suppose furthermore that $\bar{F}(x) = \lim_{T \rightarrow \infty} \frac{1}{T} \sum_{t=1}^T F_t(x)$ exists for all $x \in \mathbb{R}$ and that the limit function is strictly increasing on \mathbb{R} . Then

$$\hat{G}_T(x) = \frac{1}{T} \sum_{t=1}^T \mathbf{1}\{x_t \leq x\} \longrightarrow \bar{F}(x) \quad \text{almost surely for all } x \in \mathbb{R} \quad (9)$$

if and only if $(F_t)_{t=1,2,\dots}$ is marginally calibrated with respect to $(G_t)_{t=1,2,\dots}$.

The most obvious graphical device is a plot of $\hat{G}_T(x)$ and $\bar{F}_T(x)$ versus x . However, it is often more instructive to plot the difference of the two cumulative distribution functions, as in the left-hand side of Figure 4 which shows the difference

$$\bar{F}_T(x) - \hat{G}_T(x), \quad x \in \mathbb{R} \quad (10)$$

for the various forecasters in our initial simulation study. We call this type of display a *marginal calibration plot*. Under the hypothesis of marginal calibration, we expect minor fluctuations about zero only, and this is indeed the case for the perfect forecaster and the climatological forecaster. The unfocused forecaster and Hamill's forecaster lack marginal calibration, resulting in major excursions from zero. The same information can be visualized in terms of quantiles, as on the right-hand side of Figure 4 which shows the difference,

$$Q(\bar{F}_T, q) - Q(\hat{G}_T, q), \quad q \in (0, 1) \quad (11)$$

of the quantile functions for \bar{F}_T and \hat{G}_T , respectively. Under the hypothesis of marginal calibration, we again expect minor fluctuations about zero only, and this is the case for the perfect forecaster and the climatological forecaster. The unfocused forecaster and Hamill's forecaster show quantile difference functions that increase from negative to positive values, thereby indicating forecast climates that are too spread out.

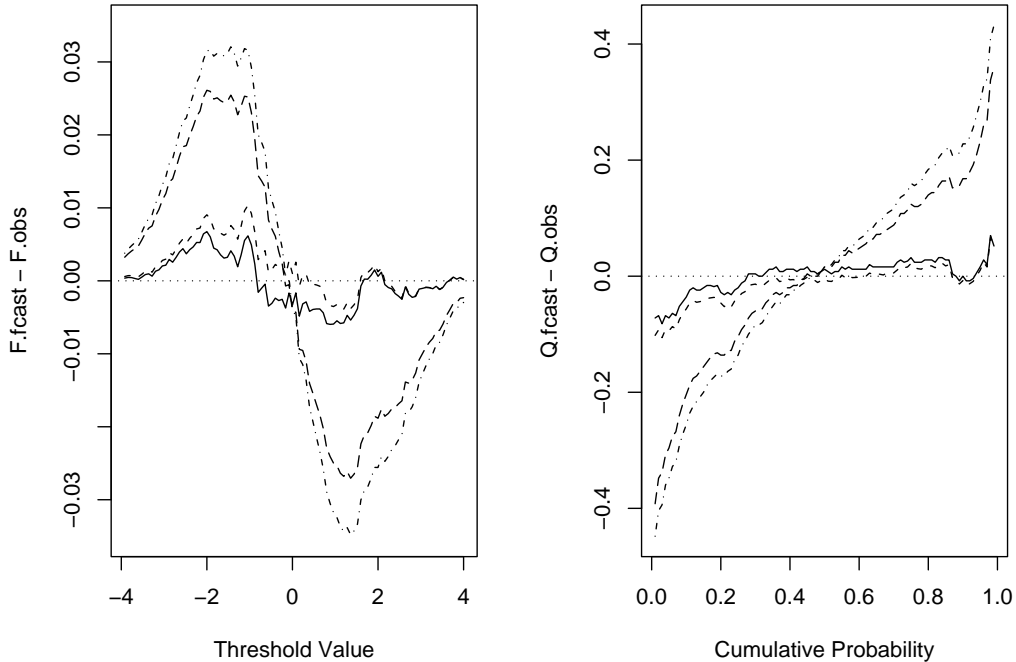


Figure 4: Marginal calibration plot for the perfect forecaster (solid line), climatological forecaster (short dashes), unfocused forecaster (dot-dashed line) and Hamill’s forecaster (long dashes). The presentation is in terms of cumulative distribution functions (left) and in terms of quantiles (right), respectively.

3.3 Assessing sharpness

Sharpness refers to the concentration of the predictive distributions and is a property of the forecasts only. The more concentrated the predictive distributions, the sharper the forecasts, and the sharper the better, subject to calibration. To assess sharpness, we use numerical and graphical summaries of the width of the associated prediction intervals. For instance, Table 4 shows the average width of the central 50% and 90% prediction intervals for the forecasters in our simulation study. The perfect forecaster is the sharpest, followed by Hamill’s forecaster, the unfocused forecaster and the climatological forecaster. A fair comparison requires that the empirical coverage of the prediction intervals be close to nominal, which we showed to be true in Figure 1 and Table 3. In our simplistic simulation study, the width of the prediction intervals is fixed, except for Hamill’s forecaster, and the tabulation is perfectly adequate. In many types of applications, however, conditional heteroscedasticity leads to considerable variability in the width of the prediction intervals. The average width then is often insufficient to characterize sharpness, and we follow Bremnes (2004) in proposing boxplots as a more instructive graphical device. The resulting *sharpness diagram* is an important diagnostic tool, and we present an example thereof in Section 4 below.

Table 4: Average width of central prediction intervals. The nominal coverages are 50% and 90%, respectively.

Interval	50%	90%
Perfect forecaster	1.35	3.29
Climatological forecaster	1.91	4.65
Unfocused forecaster	1.52	3.68
Hamill's forecaster	1.49	3.62

Table 5: Average logarithmic score (LogS) and continuous ranked probability score (CRPS).

	LogS	CRPS
Perfect forecaster	1.41	0.56
Climatological forecaster	1.75	0.78
Unfocused forecaster	1.53	0.63
Hamill's forecaster	1.52	0.61

3.4 Proper scoring rules

Scoring rules assign numerical scores to probabilistic forecasts and form attractive summary measures of predictive performance, in that they address calibration and sharpness simultaneously. We write $S(F, x)$ for the score assigned when the forecaster issues the predictive distribution F and x materializes, and we take scores to be penalties that the forecaster wishes to minimize on average. A scoring rule is *proper* if the expected value of the penalty $S(F, x)$ for an observation x drawn from G is minimized if the forecast is perfect, that is, if $F = G$. It is *strictly proper* if the minimum is unique. Propriety is a crucial characteristic of scoring rules; it rewards perfect forecasts and discourages hedging. Winkler (1977) gave an interesting discussion of the ways in which proper scoring rules encourage sharp forecasts.

The *logarithmic score* is the negative of the logarithm of the predictive density evaluated at the observation (Good 1952; Bernardo 1979). The logarithmic score is proper and has many desirable properties (Roulston and Smith 2002) yet lacks robustness (Selten 1998; Gneiting and Raftery 2004). The *continuous ranked probability score* is defined directly in terms of the predictive cumulative distribution function, F , namely as

$$\text{crps}(F, x) = \int_{-\infty}^{\infty} (F(y) - \mathbf{1}(y \geq x))^2 dy, \tag{12}$$

and provides a more robust alternative. Gneiting and Raftery (2004) gave an alternative representation and showed that

$$\text{crps}(F, x) = \mathbb{E}_F |X - x| - \frac{1}{2} \mathbb{E}_F |X - X'|, \tag{13}$$

where X and X' are independent copies of a random variable with distribution function F and finite first moment. The representation (13) shows that the continuous ranked probability score generalizes the absolute error, to which it reduces if F is a point forecast. Furthermore, it can be

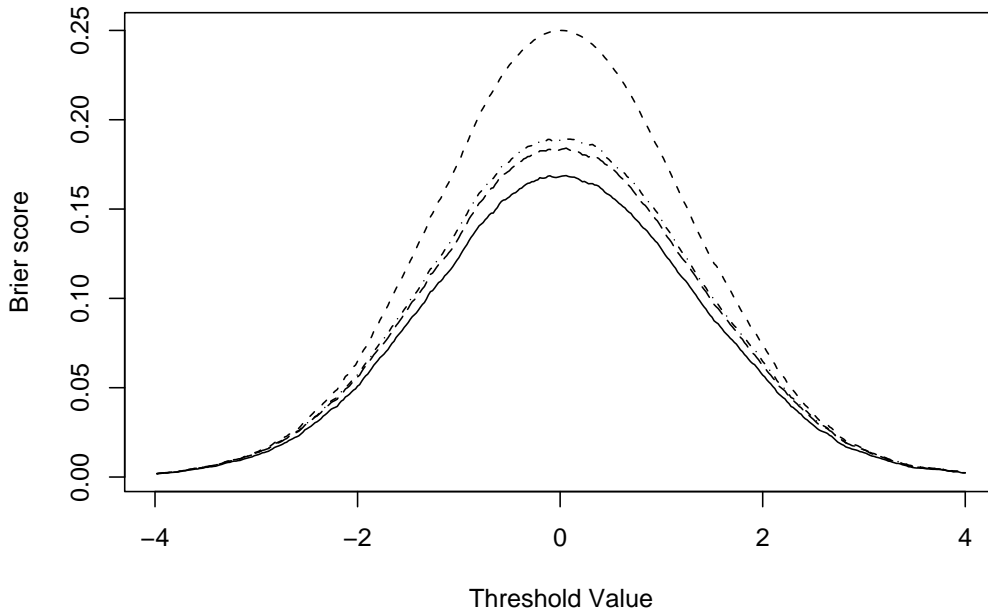


Figure 5: Brier score plot for the perfect forecaster (solid line), climatological forecaster (short dashes), unfocused forecaster (dot-dashed line), and Hamill’s forecaster (long dashes). The graphs show the Brier score as a function of the threshold value. The area under the associated curve equals the CRPS value (14).

reported in the same unit as the observations. The continuous ranked probability score is proper, and we rank competing forecast procedures based on its average,

$$\text{CRPS} = \frac{1}{T} \sum_{t=1}^T \text{crps}(F_t, x_t) = \int_{-\infty}^{\infty} \text{BS}(y) \, dy, \quad (14)$$

where $\text{BS}(y) = \frac{1}{T} \sum_{t=1}^T (F_t(y) - \mathbf{1}\{x_t \leq y\})^2$ denotes the Brier score (Brier 1950) for probability forecasts of the binary events at the threshold value $y \in \mathbb{R}$. The Brier score allows for the distinction of a calibration component and a refinement component (Murphy 1972; Blattenberger and Lad 1985), but the decomposition requires a binning of the forecast probabilities and may not be stable if the binning is changed.

Table 5 shows the logarithmic score and the continuous ranked probability score for the various forecasters in our initial simulation study, when averaged over the 10000 replicates of the prediction experiment. As expected, both scoring rules rank the perfect forecaster highest, followed by Hamill’s forecaster, the unfocused forecaster and the climatological forecaster. Figure 5 plots the Brier score for the associated binary forecasts in dependence on the threshold value, thereby illustrating the integral representation on the right-hand side of (14). This type of display was proposed by Gerds (2002, Section 2.3) and Schumacher, Graf and Gerds (2003) who called the graphs prediction error curves.

4 Case study: Probabilistic forecasts at the Stateline wind energy center

Wind power is the fastest-growing energy source today. Estimates are that within the next 15 years wind energy will fill about 6% of the electricity supply in the United States. In Denmark, wind energy already meets 20% of the country's total energy needs. However, arguments against the proliferation of wind energy have been put forth, often focusing on the perceived inability to forecast wind resources with any degree of accuracy. The development of advanced probabilistic forecast methodologies helps address these concerns.

The prevalent approach to short-range forecasts of wind speed and wind power at prediction horizons up to a few hours uses on-site observations and autoregressive time series models (Brown, Katz and Murphy 1984). Gneiting, Larson, Westrick, Genton and Aldrich (2004) proposed a novel spatio-temporal approach, the *regime-switching space-time* or RST method, that merges meteorological and statistical expertise to obtain fully probabilistic forecasts of wind resources. Henceforth, we illustrate our diagnostic approach to the evaluation of predictive distributions by a comparison and ranking of three competing forecast methodologies for two-step ahead predictions of hourly average wind speed at the Stateline wind energy center in the US Pacific Northwest. The evaluation period is May through November 2003, resulting in a total of 5136 probabilistic forecasts.

4.1 Predictive distributions for hourly average wind speed

We consider three competing statistical prediction algorithms for two-step ahead probabilistic forecasts of hourly average wind speed, w_t , at a meteorological tower in close vicinity of the Stateline wind energy center, which is located on the Vansycle ridge at the border between the states of Oregon and Washington. The data source is described in Gneiting et al. (2004).

The first method is the persistence forecast, a naive yet surprisingly skillful, nonparametric reference forecast. The persistence point forecast is simply the most recent observed value of hourly average wind speed at Stateline. To obtain a predictive distribution, we dress the point forecast with the 19 most recent observed values of the persistence error, which corresponds to a naive version of the approach of Roulston and Smith (2003). Hence, the predictive cumulative distribution function for w_{t+2} is the empirical distribution function of the set

$$\{\max(w_t - w_{t-h} + w_{t-h-2}, 0) : h = 0, \dots, 18\},$$

and the associated prediction intervals are readily formed from the order statistics of this set. The second technique is the autoregressive time series approach which was proposed by Brown, Katz and Murphy (1984) and has found widespread use since. To apply this technique, we fit and extract a diurnal trend component based on a sliding 40-day training period, fit a stationary autoregression to the residual component and find a Gaussian predictive distribution in the customary way. The Gaussian predictive distribution assigns a typically small positive mass to the negative half-axis, and in view of the nonnegativity of the predictand we redistribute this mass to wind speed zero. The details are described in Gneiting et al. (2004), where the method is referred to as the AR-D technique.

The third method is the regime-switching space-time (RST) approach of Gneiting et al. (2004). The RST model is parsimonious, yet takes account of all the salient features of wind speed: alternating atmospheric regimes, temporal and spatial autocorrelation, diurnal and seasonal non-

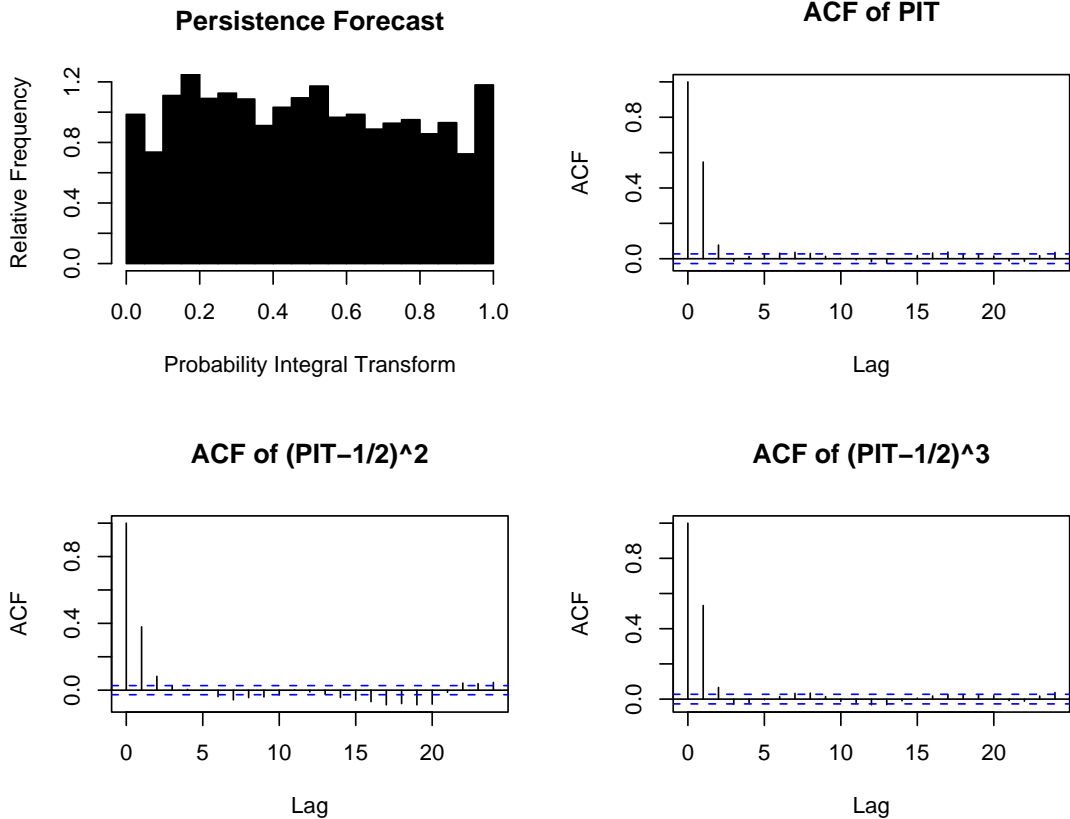


Figure 6: Probability integral transform (PIT) histogram and sample autocorrelation functions for the first three centered moments, for persistence forecasts of hourly average wind speed at the Stateline wind energy center.

stationarity, conditional heteroscedasticity and non-Gaussianity. The method utilizes offsite information from the nearby meteorological towers at Goodnoe Hills and Kennewick, identifies atmospheric regimes at the wind energy site and fits conditional predictive models for each regime, based on a sliding 45-day training period. Details are given in Gneiting et al. (2004), where the method is referred to as the RST-D-CH technique. Any minor discrepancies in the performance measures reported henceforth and in Gneiting et al. (2004) stem from the use of R versus SPLUS and the associated slight differences in the optimization algorithms used for estimating the predictive models.

4.2 Assessing calibration

Figures 6, 7 and 8 show the probability integral transform (PIT) histograms for the three forecast techniques, along with the sample autocorrelation functions for the first three centered moments of the PIT values and the associated Bartlett confidence intervals. The PIT histograms for the persistence forecasts and for the RST forecasts appear uniform. The histogram for the autoregressive forecasts is hump shaped, thereby suggesting departures from probabilistic calibration. Table 6 shows the associated empirical coverage of the 50% and 90% central prediction intervals.

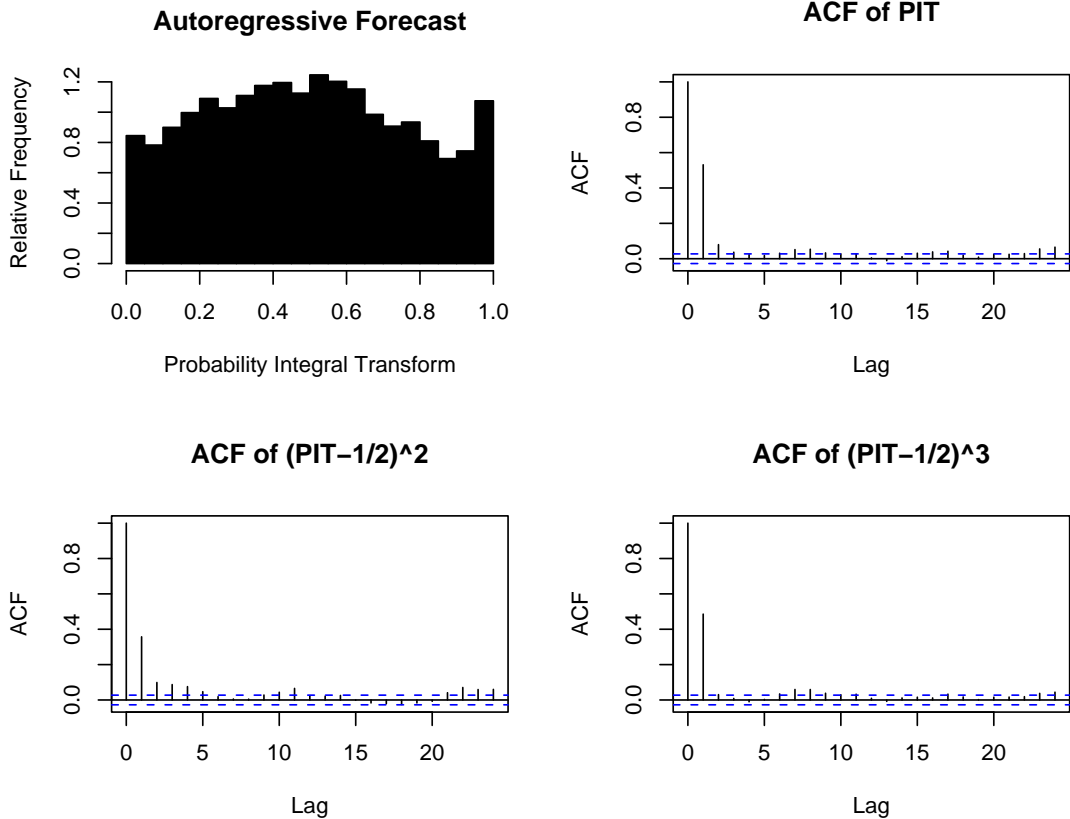


Figure 7: Same as Figure 6, but for autoregressive forecasts.

The PIT values for perfect 2-step ahead forecasts are at most 1-dependent, and the sample autocorrelation functions for the RST forecasts seem compatible with this assumption. The sample autocorrelations for the persistence forecasts are nonnegligible at lag 2, and the centered second moment of the PIT values shows notable negative correlations at lags between 15 and 20 hours. These features indicate a lack of fit of the predictive model but seem hard to interpret diagnostically. The respective sample autocorrelations for the autoregressive forecasts are positive and nonnegligible at lags up to 5 hours, thereby pointing at conditional heteroscedasticity in the wind speed series. Indeed, Gneiting et al. (2004) showed that the autoregressive forecasts improve when a conditionally heteroscedastic model is employed. In the current, classical autoregressive formulation the predictive variance varies as a result of the sliding training period, but high-frequency changes in the predictability are not taken into account.

Figure 9 shows marginal calibration plots for the three forecasts, both in terms of cumulative distribution functions and in terms of quantiles. The display is in analogy to Figure 4 and the graphs show the differences defined in (10) and (11), respectively. The graphs for all three forecasts show nonnegligible excursions from zero, particularly at small wind speeds, and the excursions are most pronounced for the autoregressive forecasts. The lack of predictive model fit can be explained by a closer examination of Figure 10, which shows the empirical cumulative distribution function, \bar{F}_T , of hourly average wind speed during the evaluation period. Hourly average wind

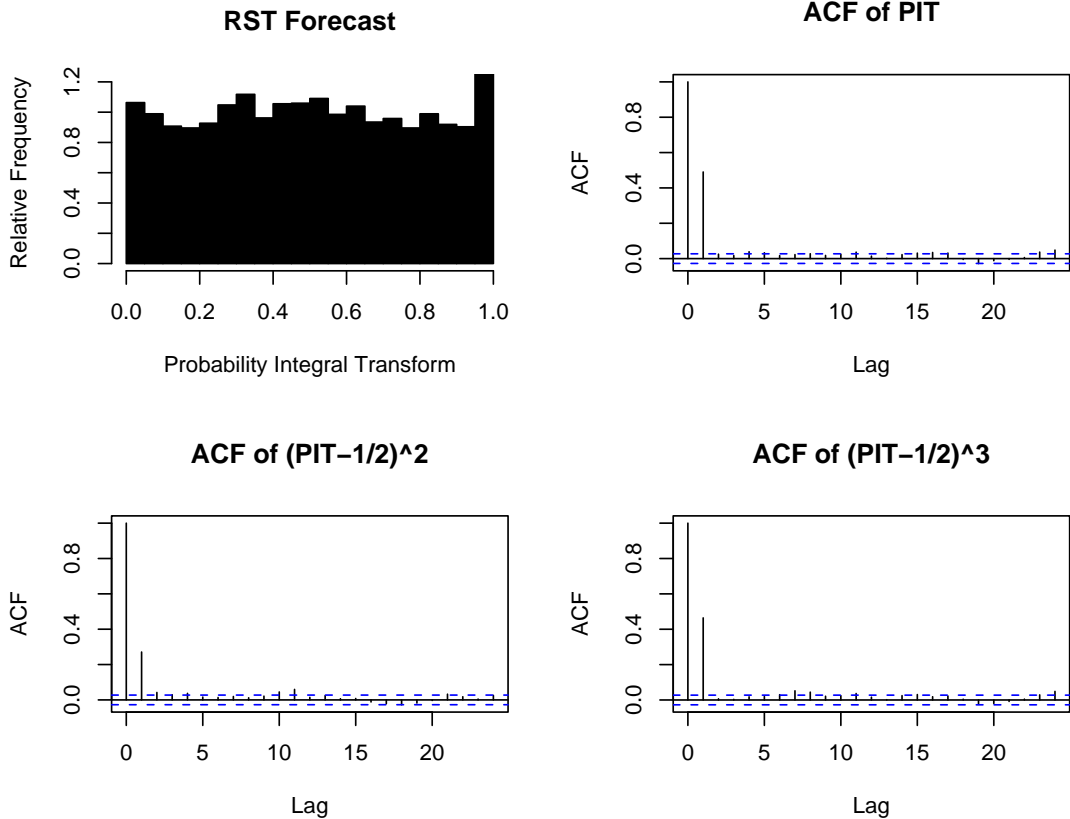


Figure 8: Same as Figure 6, but for RST forecasts.

speeds less than $1 \text{ m} \cdot \text{s}^{-1}$ were almost never observed. This is incompatible with the mean predictive distribution functions, \hat{G}_T , for the three methods, each of which assigns positive point mass to wind speed zero, resulting in the initial positive excursions in the left-hand plot of Figure 9. This issue applies to all three techniques, and for the persistence forecasts and the autoregressive forecasts it is not clear how it could be addressed. The RST method fits cut-off normal predictive distributions that are concentrated on the nonnegative half-axis and involve a point mass at zero. The marginal calibration plot suggests the use of truncated normal predictive distributions as a promising alternative.

4.3 Assessing sharpness

Sharpness concerns the concentration of the predictive distributions, and we consider the central prediction interval at the 50% and 90% level, respectively. Table 6 shows that the empirical coverage is close to nominal for all three techniques; hence, an assessment of the sharpness of the predictive distributions in terms of the width of the prediction intervals is fair. The boxplots in the sharpness diagram of Figure 11 show the 5th, 25th, 50th, 75th and 95th percentile of the width of the interval for the 5136 predictive distributions during the evaluation period, and Table 7 shows the associated average width. The prediction intervals for the persistence forecasts vary the most in width, followed by the RST forecasts and the autoregressive forecasts. The RST forecasts are

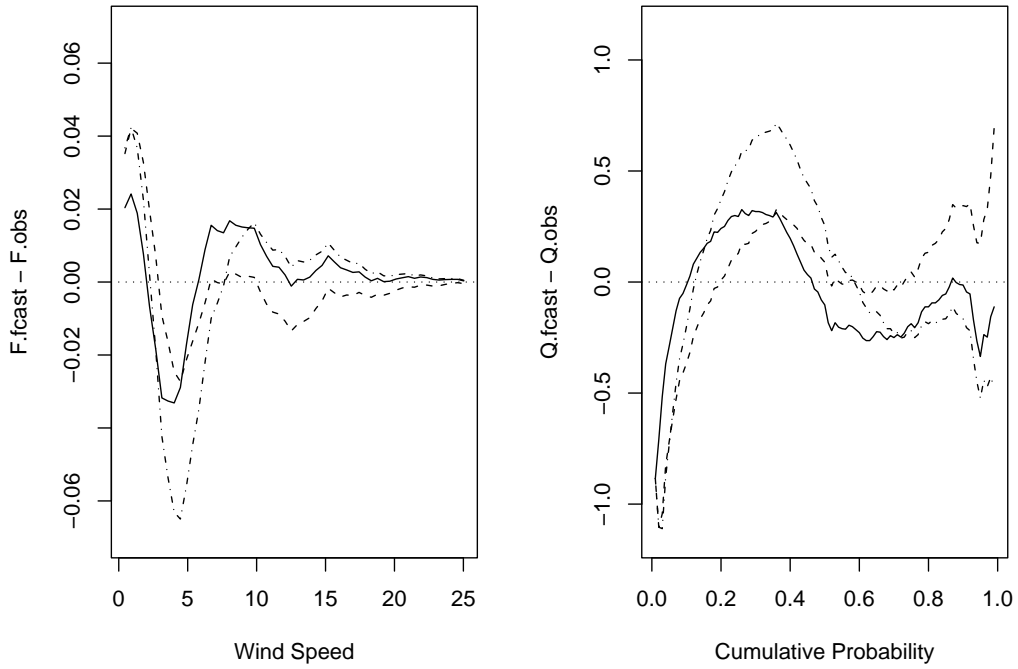


Figure 9: Marginal calibration plot for persistence forecasts (dashed line), autoregressive forecasts (dot-dashed line) and RST forecasts (solid line) of hourly average wind speed at the Stateline wind energy center in terms of cumulative distribution functions (left) and in terms of quantiles (right), respectively, in $\text{m} \cdot \text{s}^{-1}$.

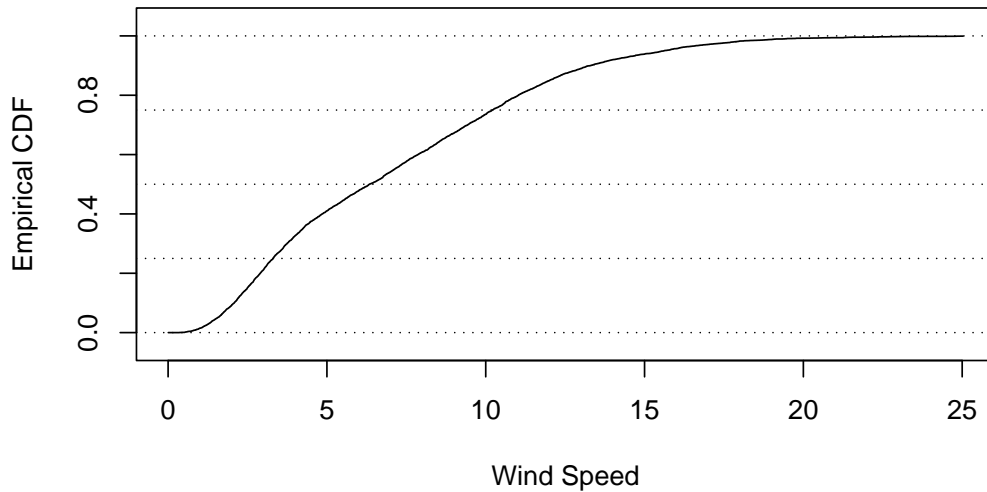


Figure 10: Empirical cumulative distribution function of hourly average wind speed at the Stateline wind energy center in May through November 2003, in $\text{m} \cdot \text{s}^{-1}$.

Table 6: Empirical coverage of central prediction intervals. The nominal coverages are 50% and 90%, respectively.

Interval	50%	90%
Persistence forecast	50.9%	89.2%
Autoregressive forecast	55.6%	90.4%
RST forecast	51.2%	88.4%

clearly the sharpest, with prediction intervals that are about 20% shorter on average than those for the autoregressive forecasts.

4.4 Continuous ranked probability score

Table 8 shows the mean continuous ranked probability score or CRPS value (14) for the various forecasts. We report the scores month by month, which allows for an assessment of seasonal effects and straightforward tests of the null hypothesis of no difference in the predictive performance of competing probabilistic forecasts. For instance, the RST forecasts had a lower CRPS value than the autoregressive forecasts in each month during the evaluation period, May through November 2003. Under the null hypothesis of equal predictive performance this happens with probability $(\frac{1}{2})^7 = \frac{1}{128}$ only. Similarly, the autoregressive forecasts outperformed the persistence forecasts in May through October 2003, but not in November 2003. Clearly, various other tests can be employed, but one needs to be careful to avoid dependencies in the forecast differentials. In our situation, the results for distinct months can be considered independent for all practical purposes. Diebold and Mariano (1995) gave a thoughtful discussion of these issues, and we refer to their work for a comprehensive account of tests of predictive performance. Figure 12 illustrates the Brier score decomposition (14) of the CRPS value for the entire evaluation period. The RST forecasts outperform the persistence forecasts and the autoregressive forecasts at all thresholds.

We noted in Section 3.4 that the continuous ranked probability score generalizes the absolute error, and reduces to the latter for point forecasts. Table 9 shows the mean absolute error (MAE) for the point forecasts associated with the persistence, autoregressive and RST techniques, respectively. The persistence point forecast is simply the most recent observed value of the hourly average wind speed at the Stateline wind energy center. The autoregressive point forecast is the mean of the associated predictive distribution, and similarly for the RST forecast. The results for the predictive median are very similar. The RST point forecasts outperform the autoregressive point forecasts, and the autoregressive point forecasts outperform the persistence point forecasts. The MAE values in Table 9 and the CRPS values in Table 8 are reported in the same unit as the wind speed measurements, that is, in $\text{m} \cdot \text{s}^{-1}$, and can be directly compared. The insights that the monthly scores provide are indicative of the potential benefits of thoughtful stratification.

The CRPS and MAE values establish a clear-cut ranking of the competing forecast methodologies that places the RST technique first, followed by the autoregressive and the persistence forecasts. The RST method also performed best in terms of probabilistic calibration and marginal calibration, and the RST forecasts were much sharper than the autoregressive and the persistence forecasts. The diagnostic approach furthermore points at forecast deficiencies and suggests potential improvements to the predictive models. In particular, the marginal calibration plots in Figure

Table 7: Average width of central prediction intervals, in $\text{m} \cdot \text{s}^{-1}$. The nominal coverages are 50% and 90%, respectively.

Interval	50%	90%
Persistence forecast	2.63	7.51
Autoregressive forecast	2.74	6.55
RST forecast	2.20	5.31

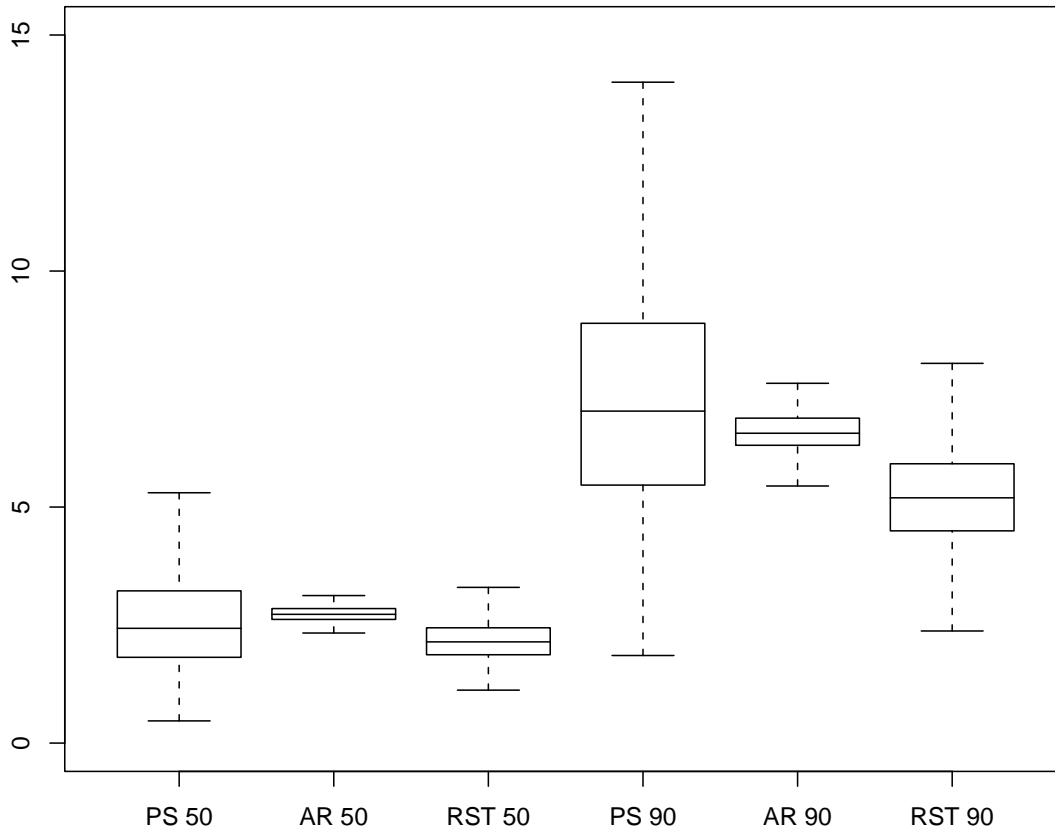


Figure 11: Sharpness diagram for persistence forecasts (PS), autoregressive forecasts (AR) and RST forecasts of hourly average wind speed at the Stateline wind energy center. The boxplots show the 5th, 25th, 50th, 75th and 95th percentile of the width of the central prediction interval, in $\text{m} \cdot \text{s}^{-1}$. The nominal coverage is 50% and 90%, respectively.

Table 8: Average continuous ranked probability score (CRPS) for probabilistic forecasts of hourly average wind speed at the Stateline wind energy center in March through November 2003, month by month and for the entire evaluation period, in $\text{m} \cdot \text{s}^{-1}$.

CRPS	May	Jun	Jul	Aug	Sep	Oct	Nov	Mar–Nov
Persistence forecast	1.16	1.08	1.29	1.21	1.20	1.29	1.16	1.20
Autoregressive forecast	1.12	1.02	1.10	1.11	1.11	1.22	1.13	1.12
RST forecast	0.96	0.85	0.95	0.95	0.97	1.08	1.00	0.97

Table 9: Mean absolute error (MAE) for point forecasts of hourly average wind speed at the Stateline wind energy center in March through November 2003, month by month and for the entire evaluation period, in $\text{m} \cdot \text{s}^{-1}$.

MAE	May	Jun	Jul	Aug	Sep	Oct	Nov	Mar–Nov
Persistence forecast	1.60	1.45	1.74	1.68	1.59	1.68	1.51	1.61
Autoregressive forecast	1.53	1.38	1.50	1.54	1.53	1.68	1.54	1.53
RST forecast	1.32	1.18	1.33	1.31	1.36	1.48	1.37	1.34

9 suggest a modified version of the RST technique that uses truncated normal rather than cut-off normal predictive distributions. This modification yields small but consistent improvements in the predictive performance of the RST method, and we intend to report details in subsequent work.

5 Discussion

Our paper addressed the important issue of evaluating predictive performance for probabilistic forecasts of continuous variables. Following the lead of Dawid (1984) and Diebold, Gunther and Tay (1998), predictive distributions have traditionally been evaluated within the framework of checks for perfect forecasts, consisting of an assessment on the uniformity and independence of the probability integral transform. We introduced the more pragmatic and flexible paradigm of *maximizing sharpness subject to calibration*. Calibration refers to the statistical consistency between the predictive distributions and the associated observations and is a joint property of the predictions and the values that materialize. Sharpness refers to the concentration of the predictive distributions and is a property of the forecasts only.

We interpreted probabilistic forecasting within a game-theoretic framework that allowed us to distinguish probabilistic calibration, exceedance calibration and marginal calibration, and we developed diagnostic tools for evaluating and comparing probabilistic forecasters. Probabilistic calibration corresponds to the uniformity of the probability integral transform (PIT), and the PIT histogram remains a key tool in the diagnostic approach to forecast evaluation. In addition, we proposed the use of marginal calibration plots, sharpness diagrams and proper scoring rules, which form powerful tools for learning about forecast deficiencies and ranking competing forecast methodologies. Our own applied work on probabilistic forecasting has benefitted immensely from these tools, as documented in Section 4 and in the partial applications in Gneiting et al. (2004), Raftery, Gneiting, Balabdaoui and Polakowski (2005) and Gneiting et al. (2005). Furthermore,

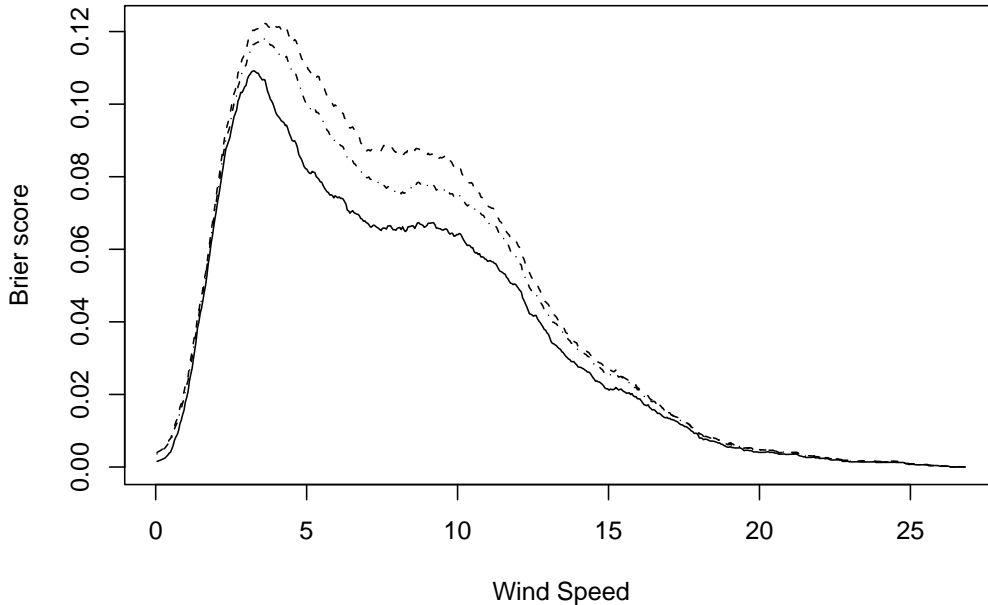


Figure 12: Brier score plot for persistence forecasts (dashed line), autoregressive forecasts (dot-dashed line) and RST forecasts (solid line) of hourly average wind speed at the Stateline wind energy center, in $\text{m}\cdot\text{s}^{-1}$. The graphs show the Brier score as a function of the threshold value. The area under the associated curve equals the CRPS value (14).

predictive distributions can be reduced to point forecasts, or to probability forecasts of binary events, and the associated forecasts can be assessed using the diagnostic devices described by Murphy, Brown and Chen (1989) and Murphy and Winkler (1992), among others.

If we were to reduce our conclusions to a single recommendation, we would close with a call for the assessment of sharpness, particularly when the goal is that of ranking. Previous comparative studies of the predictive performance of probabilistic forecasts have largely focused on calibration. For instance, Moyeed and Papritz (2002) compared spatial prediction techniques, Clements and Smith (2000) and Boero and Marrocu (2004) evaluated linear and non-linear time series models, Garrat et al. (2003) assessed macroeconomic forecast models, and Bauwens et al. (2004) studied the predictive performance of financial duration models. In each of these works, the assessment took place in terms of the predictive performance of the associated point forecasts, and in terms of the uniformity of the probability integral transform. We contend that comparative studies of these types call for routine assessments of sharpness, in the form of sharpness diagrams and through the use of proper scoring rules.

Despite the frequentist flavor of our diagnostic approach, calibration and sharpness are properties that are relevant to Bayesian forecasters as well. Rubin (1984, pp. 1161 and 1160) noted that “the probabilities attached to Bayesian statements do have frequency interpretations that tie the statements to verifiable real world events.” Consequently, a “Bayesian is calibrated if his probability statements have their asserted coverage in repeated experience.” Gelman, Meng and Stern

(1996) developed Rubin's posterior predictive approach, proposed posterior predictive checks as Bayesian counterparts to the classical tests for goodness of fit, and advocated their use in judging the fit of Bayesian models. This relates to our diagnostic approach, which emphasizes the need for understanding the ways in which predictive distributions fail or succeed. Indeed, the diagnostic devices posited herein form powerful tools for Bayesian as well as frequentist model diagnostics and model choice. Tools such as the PIT histogram, marginal calibration plots, sharpness diagrams and proper scoring rules are widely applicable, since they are nonparametric, do not depend on nested models, allow for structural change, and apply to predictive distributions that are represented by samples, as they arise in a rapidly growing number of Markov chain Monte Carlo methodologies and ensemble prediction systems. In the time series context, the predictive framework is natural and the model fit can be assessed through the performance of the time-forward predictive distributions (Smith 1985; Shephard 1994; Frühwirth-Schnatter 1996; Bouwens et al. 2004). In other types of situations, a cross-validatory approach can often be used fruitfully (Dawid 1984a, p. 288; Gneiting and Raftery 2004).

Appendix

Proof of Theorem 1

Consider the random variable $U = F(x_1)^{z_1} F(x_2)^{z_2} \cdots F(x_T)^{z_T}$ where $x_1 \sim G_1, \dots, x_T \sim G_T$ and $(z_1, \dots, z_T)'$ is multinomial with equal probabilities. The finite probabilistic calibration condition implies that U is uniformly distributed. By the variance decomposition formula,

$$\text{var}(F) = \text{var}(F^{-1}(U)) = \mathbb{E} \left[\text{var} \left(F^{-1}(U) \mid z_1, \dots, z_T \right) \right] + \text{var} \left[\mathbb{E} \left(F^{-1}(U) \mid z_1, \dots, z_T \right) \right].$$

The first term in the decomposition equals

$$\frac{1}{T} \sum_{t=1}^T \text{var}(x_t) = \frac{1}{T} \sum_{t=1}^T \text{var}(G_t)$$

and the second term is nonnegative and vanishes if and only if $\mathbb{E}(G_1) = \cdots = \mathbb{E}(G_T)$. ■

Proof of Theorem 2

For $p \in (0, 1)$ and $t = 1, 2, \dots$, put $Y_t = \mathbf{1}\{p_t < p\} - G_t \circ F_t^{-1}(p)$ and note that $\mathbb{E}(Y_t) = 0$. By Theorem 2 of Blum et al. (1963),

$$\lim_{T \rightarrow \infty} \frac{1}{T} \sum_{t=1}^T Y_t = \lim_{T \rightarrow \infty} \frac{1}{T} \sum_{t=1}^T \left(\mathbf{1}\{p_t < p\} - G_t \circ F_t^{-1}(p) \right) = 0$$

almost surely. The uniqueness of the limit implies that (6) is equivalent to the probabilistic calibration condition (3). ■

Proof of Theorem 3

For $x \in \mathbb{R}$ let $q = \bar{F}(x)$, and for $t = 1, 2, \dots$ put $q_t = \bar{F}(x_t)$. Then

$$\hat{G}_T(x) = \frac{1}{T} \sum_{t=1}^T \mathbf{1}\{x_t \leq x\} = \frac{1}{T} \sum_{t=1}^T \mathbf{1}\{q_t \leq q\}.$$

By Theorem 2 with $F_t = \bar{F}$ for $t = 1, 2, \dots$ we have that $\frac{1}{T} \sum_{t=1}^T \mathbf{1}\{q_t \leq q\} \rightarrow q$ almost surely if and only if $\frac{1}{T} \sum_{t=1}^T G_t \circ \bar{F}^{-1}(q) \rightarrow q$ almost surely; hence, marginal calibration is equivalent to (9). ■

Acknowledgements

We thank Barbara G. Brown, Hans R. Künsch, Kristin Larson, Jon A. Wellner, Anton H. Westveld and Kenneth Westrick for discussions, comments and references. Our work has been supported by the DoD Multidisciplinary University Research Initiative (MURI) program administered by the Office of Naval Research under Grant N00014-01-10745. Tilmann Gneiting also acknowledges support by the National Science Foundation under Award no. 0134264 and by the Washington Technology Center.

References

- Anderson, J. L. (1996), A method for producing and evaluating probabilistic forecasts from ensemble model integrations, *Journal of Climate*, **9**, 1518–1530.
- Bauwens, L., Giot, P., Grammig, J. and Veredas, D. (2004), A comparison of financial duration models via density forecasts, *International Journal of Forecasting*, **20**, 589–609.
- Berkowitz, J. (2001), Testing density forecasts, with applications to risk management, *Journal of Business and Economic Statistics*, **19**, 465–474.
- Bernardo, J. M. (1979), Expected information as expected utility, *Annals of Statistics*, **7**, 686–690.
- Besag, J., Green, P., Higdon, D. and Mengersen, K. (1995), Bayesian computing and stochastic systems (with discussion and rejoinder), *Statistical Science*, **10**, 3–66.
- Blattenberger, G. and Lad, F. (1985), Separating the Brier score into calibration and refinement components: A graphical exposition, *American Statistician*, **39**, 26–32.
- Blum, J. R., Hanson, D. L. and Koopmans, L. H. (1963), On the strong law of large numbers for a class of stochastic processes, *Zeitschrift für Wahrscheinlichkeitstheorie und verwandte Gebiete*, **2**, 1–11.
- Boero, G. and Marrocu, E. (2004), The performance of SETAR models: a regime conditional evaluation of point, interval and density forecasts, *International Journal of Forecasting*, **20**, 305–320.
- Bremnes, J. B. (2004), Probabilistic forecasts of precipitation in terms of quantiles using NWP model output, *Monthly Weather Review*, **132**, 338–347.
- Brier, G. W. (1950), Verification of forecasts expressed in terms of probability, *Monthly Weather Review*, **78**, 1–3.
- Brown, B. G., Katz, R. W. and Murphy, A. H. (1984), Time series models to simulate and forecast wind speed and wind power, *Journal of Climate and Applied Meteorology*, **23**, 1184–1195.
- Campbell, S. D. and Diebold, F. X. (2005), Weather forecasting for weather derivatives, *Journal of the American Statistical Association*, **100**, 6–16.
- Christoffersen, P. F. (1998), Evaluating interval forecasts, *International Economic Review*, **39**, 841–862.

- Clements, M. P. and Smith, J. (2000), Evaluating the forecast densities of linear and non-linear models: Applications to output growth and unemployment, *Journal of Forecasting*, **19**, 255–276.
- Dawid, A. P. (1982), The well-calibrated Bayesian, *Journal of the American Statistical Association*, **77**, 605–610.
- Dawid, A. P. (1984), Statistical theory: The prequential approach (with discussion), *Journal of the Royal Statistical Society Ser. A*, **147**, 278–292.
- Dawid, A. P. (1985a), The impossibility of inductive inference, *Journal of the American Statistical Association*, **80**, 340–341.
- Dawid, A. P. (1985b), Calibration-based empirical probability (with discussion and rejoinder), *Annals of Statistics*, **13**, 1251–1285.
- Diebold, F. X. and Mariano, R. S. (1995), Comparing predictive accuracy, *Journal of Business and Economic Statistics*, **13**, 253–263.
- Diebold, F. X., Gunther, T. A. and Tay, A. S. (1998), Evaluating density forecasts with applications to financial risk management, *International Economic Review*, **39**, 863–883.
- Duffie, D. and Pan, J. (1997), An overview of value at risk, *Journal of Derivatives*, **4**, 7–49.
- Foster, D. P. and Vohra, R. V. (1998), Asymptotic calibration, *Biometrika*, **85**, 379–390.
- Frühwirth-Schnatter, S. (1996), Recursive residuals and model diagnostics for normal and non-normal state space models, *Environmental and Ecological Statistics*, **3**, 291–309.
- Garratt, A., Lee, K., Pesaran, M. H. and Shin, Y. (2003), Forecast uncertainties in macroeconomic modelling: An application to the UK economy, *Journal of the American Statistical Association*, **98**, 829–838.
- Gelman, A., Meng, X.-L. and Stern, H. (1996), Posterior predictive assessment of model fitness via realized discrepancies, *Statistica Sinica*, **6**, 733–807.
- Gerds, T. (2002), Nonparametric efficient estimation of prediction error for incomplete data models, Ph. D. Thesis, Mathematische Fakultät, Albert-Ludwigs-Universität Freiburg, Freiburg, Germany.
- Gneiting, T. and Raftery, A. E. (2004), Strictly proper scoring rules, prediction, and estimation, Technical Report no. 463, Department of Statistics, University of Washington, available at www.stat.washington.edu/www/research/reports.
- Gneiting, T., Raftery, A. E., Westveld, A. H. and Goldman, T. (2005), Calibrated probabilistic forecasting using ensemble model output statistics and minimum CRPS estimation, *Monthly Weather Review*, **133**, in press.
- Gneiting, T., Larson, K., Westrick, K., Genton, M. G. and Aldrich, E. (2004), Calibrated probabilistic forecasting at the Stateline wind energy center: The regime-switching space-time (RST) method, Technical Report no. 464, Department of Statistics, University of Washington, available at www.stat.washington.edu/www/research/reports.
- Good, I. J. (1952), Rational decisions, *Journal of the Royal Statistical Society Ser. B*, **14**, 107–114.
- Hamill, T. M. (2001), Interpretation of rank histograms for verifying ensemble forecasts, *Monthly Weather Review*, **129**, 550–560.
- Hamill, T. M. and Colucci, S. J. (1997), Verification of Eta-RSM short-range ensemble forecasts, *Monthly Weather Review*, **125**, 1312–1327.

- Hoeting, J. (1994), Accounting for model uncertainty in linear regression, Ph. D. Thesis, Department of Statistics, University of Washington, Seattle, Washington.
- Jolliffe, I. T. and Stephenson, D. B., eds. (2003), *Forecast Verification. A Practitioner's Guide in Atmospheric Science*, Chichester, United Kingdom: Wiley.
- Krzysztofowicz, R. (1999), Bayesian theory of probabilistic forecasting via deterministic hydrologic model, *Water Resources Research*, **35**, 2739–2750.
- Krzysztofowicz, R. and Sigrest, A. A. (1999), Calibration of probabilistic quantitative precipitation forecasts, *Weather and Forecasting*, **14**, 427–442.
- Moyeed, R. A. and Papritz, A. (2002), An empirical comparison of kriging methods for nonlinear spatial point prediction, *Mathematical Geology*, **34**, 365–386.
- Murphy, A. H. (1972), Scalar and vector partitions of the probability score. Part I: Two-state situation, *Journal of Applied Meteorology*, **11**, 273–278.
- Murphy, A. H. and Winkler, R. L. (1987), A general framework for forecast verification, *Monthly Weather Review*, **115**, 1330–1338.
- Murphy, A. H. and Winkler, R. L. (1992), Diagnostic verification of probability forecasts, *International Journal of Forecasting*, **7**, 435–455.
- Murphy, A. H., Brown, B. G. and Chen, Y.-S. (1989), Diagnostic verification of temperature forecasts, *Weather and Forecasting*, **4**, 485–501.
- Noceti, P., Smith, J. and Hodges, S. (2003), An evaluation of tests of distributional forecasts, *Journal of Forecasting*, **22**, 447–455.
- Oakes, D. (1985), Self-calibrating priors do not exist, *Journal of the American Statistical Association*, **80**, 339.
- Palmer, T. N. (2002), The economic value of ensemble forecasts as a tool for risk assessment: From days to decades, *Quarterly Journal of the Royal Meteorological Society*, **128**, 747–774.
- Pearson, K. (1933), On a method of determining whether a sample of size n supposed to have been drawn from a parent population having a known probability integral has probably been drawn at random, *Biometrika*, **25**, 379–410.
- Raftery, A. E., Gneiting, T., Balabdaoui, F. and Polakowski, M. (2005), Using Bayesian model averaging to calibrate forecast ensembles, *Monthly Weather Review*, **133**, in press.
- Rosenblatt, M. (1952), Remarks on a multivariate transformation, *Annals of Mathematical Statistics*, **23**, 470–472.
- Roulston, M. S. and Smith, L. A. (2002), Evaluating probabilistic forecasts using information theory, *Monthly Weather Review*, **130**, 1653–1660.
- Roulston, M. S. and Smith, L. A. (2003), Combining dynamical and statistical ensembles, *Tellus*, **A55**, 16–30.
- Rubin, D. B. (1984), Bayesianly justifiable and relevant frequency calculations for the applied statistician, *Annals of Statistics*, **12**, 1151–1172.
- Schervish, M. J. (1985), Comment, *Journal of the American Statistical Association*, **80**, 341–342.
- Schervish, M. J. (1989), A general method for comparing probability assessors, *Annals of Statistics*, **17**, 1856–1879.
- Schumacher, M., Graf, E. and Gerds, T. (2003), How to assess prognostic models for survival data: A case study in oncology, *Methods of Information in Medicine*, **42**, 564–571.

- Seillier-Moiseiwitsch, F. (1993), Sequential probability forecasts and the probability integral transform, *International Statistical Review*, **61**, 395–408.
- Selten, R. (1998), Axiomatic characterization of the quadratic scoring rule, *Experimental Economics*, **1**, 43–62.
- Shephard, N. (1994), Partial non-Gaussian state space, *Biometrika*, **81**, 115–131.
- Smith, J. Q. (1985), Diagnostic checks of non-standard time series models, *Journal of Forecasting*, **4**, 283–291.
- Stael von Holstein, C.-A. S. (1970), *Assessment and Evaluation of Subjective Probability Distributions*, Stockholm, Sweden: Economics Research Institute, Stockholm School of Economics.
- Talagrand, O., Vautard, R. and Strauss, B. (1997), Evaluation of probabilistic prediction systems, in *Proceedings of a Workshop held at ECMWF on Predictability*, 20–22 October 1997, Reading, United Kingdom: European Centre for Medium-Range Weather Forecasts, pp. 1–25.
- Wallis, K. F. (2003), Chi-squared tests of interval and density forecasts, and the Bank of England’s fan charts, *International Journal of Forecasting*, **19**, 165–175.
- Weigend, A. S. and Shi, S. (2000), Predicting daily probability distributions of S&P500 returns, *Journal of Forecasting*, **19**, 375–392.
- Winkler, R. L. (1977), Rewarding expertise in probability assessment, in *Decision Making and Change in Human Affairs*, Jungermann, H. and de Zeeuw, G., eds., Dordrecht, Holland: D. Reidel, pp. 127–140.